

¹⁷D. Arnush, B. Fried, C. Kennel, K. Nishikawa, and A. Y. Wong, University of California, Los Angeles, Report No. PPG 139, 1972 (unpublished).

¹⁸C. Yamanaka, T. Yamanaka, and T. Sasaki, in "Laser Interaction and Related Phenomena," edited by H. J. Schwarz (Plenum, New York, to be published).

Convective Velocity Field in the Rayleigh-Bénard Instability: Experimental Results

P. Berge and M. Dubois

Service de Physique du Solide et de Résonance Magnétique, Centre d'Etudes Nucléaires de Saclay, 91190 Gif-sur-Yvette, France

(Received 27 November 1973)

We used the frequency analysis of the light scattered from a fluid to study the convective velocities in the Rayleigh-Bénard instability. The spatial dependence of the velocity is in agreement with theory. The behavior of the convective flow with the temperature seems to reach the predicted theoretical one only for $R > 1.5R_c$.

When a horizontal shallow layer of a quiescent fluid is submitted to a constant thermal gradient which is directed parallel to the body force (i.e., "heated from below"), the quiescent state breaks down and thermal convection sets in, provided this gradient exceeds a critical value. When the fluid is confined above and below by rigid surfaces, the convection cell patterns are rolls whose forms are dependent on the geometry of lateral walls. We have in mind standard fluids that can be described in the range of temperature under experimental considerations by the Boussinesq approximation.

Many studies, both theoretical and experimental,¹ have been devoted to this subject, usually referred to as the Bénard problem, but very little has been done about velocity measurements. The aim of this Letter is to report preliminary measurements of convective velocity near the critical instability gradient.

The local velocity of the fluid is measured with a laser velocimeter using a system of real fringes.² Two incident laser beams on the same vertical plane are sent through the fluid; they intersect at the midheight of the cell. At this crossing point they interfere, producing plane fringes parallel to the bisecting plane of the two beams, hence parallel to a horizontal plane. An elementary computation gives the separation of the fringes; in our experimental arrangement it has the value

$$i = \frac{1}{2}\lambda_0 / (n^2 - \cos^2\alpha)^{1/2}.$$

Here λ_0 is the wavelength of the incident beam in air, n is the mean value of the refractive index of the fluid, and α is half the angle of the two

beams in air.

If a particle passes through the fringes with a velocity \vec{V} making an angle θ with the vertical direction, the light scattered from this particle will be modulated with period $t = i / V \cos\theta$. In the case of a single velocity \vec{V} , the spectral analysis of the scattered intensity gives a single frequency peak at $f = t^{-1} = V \cos(\theta) / i$, or $f = V_z / i$. Notice that it is not possible to know the direction of the velocity with the "arrangement" described above; one can only measure the absolute value of its vertical component V_z . Therefore, we always made our measurements in the middle horizontal plane of the cell, where the direction of the convective velocity is supposed to be less distorted from the vertical.

In order to know if the measured vertical component V_z corresponds to an upward or to a downward motion, we can insert in the path of one of the laser beams a continuous phase shift; hence there is continuous vertical displacement of the fringes, the direction of which with respect to the body force is known. The corresponding shift of the measured frequency peak gives directly the orientation of the velocity.

The cell containing the fluid [in this case silicone oil, the viscosity η of which is equal to 1 S (stokes) at 25 C] is a rectangular box of 4.5 mm height, 100 mm length, and 60 mm width (see Fig. 1). The temperature of the upper and lower glass plates confining the oil is fixed to a desired value by two continuous water flows coming from two separate thermostats. In practice the upper plate was maintained at ~ 25 C. The vertical walls of the cell are made of glass, a much better conductor than the oil.

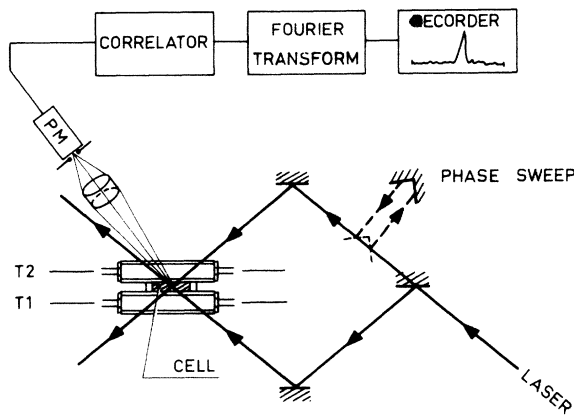


FIG. 1. Experimental arrangement.

We add to the oil a very small quantity of graphite powder. The light scattered by these particles is collected by a lens which forms the image of the cross point of the two beams on a pinhole just before the photocathode of the photomultiplier. We fix the angle between the two beams in the oil to 99° , and the effective volume in which the velocity measurements are performed is smaller than $0.5 \times 0.5 \times 0.5 \text{ mm}^3$. The spectral analysis of the photocurrent is performed by a standard correlator-Fourier-transformer system.

The shape and size of the convection pattern can be obtained by a direct observation of the graphite (or aluminum) powder. However, since in our experiment we were not interested in the cell structure, we made the concentration of such particles very low. We checked the convection patterns however through the spatial modulation of the refractive index due to the convective motions; if we illuminate the complete cell with a vertical parallel beam, we obtain excellent images of the refracted beam on a screen located at about 10 cm below the cell. One obtains directly the geometry of the rolls with photographs of these pictures. In the case of our rectangular cell, the rolls are straight, regularly spaced, and parallel to the short side of the frame.

A typical light spectrum due to convective motion in the oil is given in Fig. 2, through the analysis of the photocurrent fluctuations. The linewidth of the frequency peak is only due to instrumental resolution. Thus we can safely state that there is no dispersion of either the amplitude or the direction of the convective velocity in the effective volume of the measurement.

Figure 3 shows the variation of the vertical

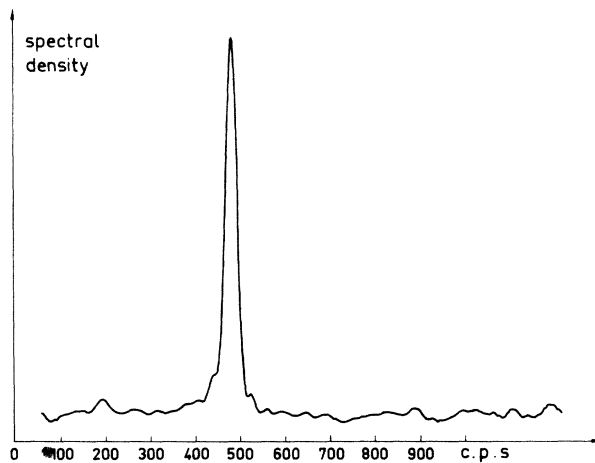


FIG. 2. Typical frequency spectrum of the photocurrent for $\Delta T > \Delta T_c$ showing the peak relative to a local convective velocity; $R \sim 2200$.

component of the velocity field, V_z , with the distance l between the point of measurement and the short side wall of the cell; l is measured perpendicular to the rolls' axis. The point of measurement is always at the midheight of the oil layer. The spatial periodicity of the rolls is shown clearly by the data and agrees with the separation of the rolls obtained from the photographs. The corresponding value of $\lambda = r/d$ is 2.18,³ where r is the wavelength of the rolls and d is the depth of the layer.

The sinusoidal behavior (shown in Fig. 3) is in excellent agreement with the theoretical prediction.⁴ On the other hand, if we move the cell parallel to its short side, without changing the posi-

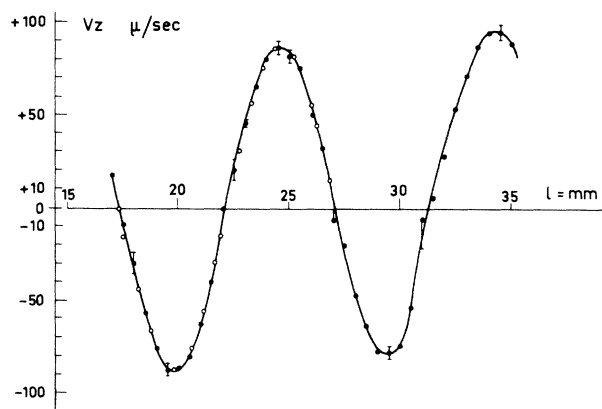


FIG. 3. Dependence of the velocity V_z on the distance l to the short side wall of the cell (measured perpendicular to the rolls' axis). Positive velocity corresponds to ascending motion; $R \sim 2000$. Open circles, calculated sinusoidal dependence.

TABLE I. Physical constants of the silicone oil used. The accuracy of the quoted physical constants is only a few percent.

$\alpha = 0.96 \times 10^{-3} \text{ deg}^{-1}$
$\eta_{25\text{C}} = 100 \text{ cS}$
$\eta_{40\text{C}} = 75 \text{ cS}$
$\chi = 1.2 \times 10^{-3} \text{ cm}^2 \text{ sec}^{-1}$
$\rho_{25\text{C}} = 0.96 \text{ g cm}^{-3}$

tion of the laser beams (l constant), the measured value of the velocity remains unchanged within the experimental error. This last result confirms once more the linear roll structure of the convection.

We also measured the variation of $V_{z \text{ max}}$ (maximum of the vertical convective velocity) with a respect to the difference $\Delta T - \Delta T_c$, where ΔT is the actual temperature difference and ΔT_c the critical one. The value of ΔT_c is determined, not by the onset of the flow pattern, but by the extrapolation at $V_z = 0$ of the curve $V_z = f(\Delta T)$. We found $\Delta T_c = 16.75^\circ$ which corresponds to a critical Rayleigh number $R_c = 1700 \pm 50$, in agreement with the theoretical value. Remember that it is convenient to express the experimental data in terms of the dimensionless Rayleigh number

$$R = \alpha g d^3 \Delta T / \eta \chi.$$

Here α is the thermal expansion coefficient, χ the thermal diffusivity, and g the gravity acceleration. The other symbols have been defined above. The values of these different parameters are summarized in Table I.

Figure 4 shows the variation of $V_{z \text{ max}}$ with respect to temperature.⁵ This behavior⁶ can be fitted with a power law such as

$$V_{z \text{ max}} \sim (R - R_c)^{0.60 \pm 0.02}. \quad (1)$$

The value of this exponent disagrees with the classical predictions.^{7,8} This disagreement may be due either to the non-Boussinesq conditions of our experiment or to the high conductivity of the side walls. We performed another set of experiments with the same fluid but we took a cell of height 10 mm constructed with Plexiglas side walls of conductivity similar to the oil. For this new geometry ($d = 10$ mm), the critical gradient is reduced to the value $\Delta T_c = 1.9$ C which corresponds to a much better approach to the Boussinesq approximation. On the other hand, the value of ΔT_c gives exactly the same critical Rayleigh number as in the first experiment. How-

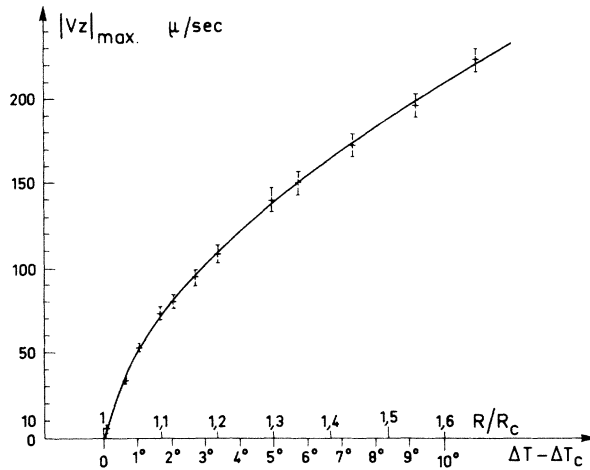


Fig. 4. Dependence of the velocity $V_{z \text{ max}}$ on temperature.

ever, the finite temperature stability of our experimental arrangement (± 0.03 C) does not allow studying with good accuracy the domain of temperature near R_c . In the domain $1.3R_c < R < 2.5R_c$, the behavior of $V_{z \text{ max}}$ varies unambiguously as $(R - R_c)^{0.55 \pm 0.02}$.

To our knowledge this is the first report on the measurement of local convective velocities near the threshold of the Rayleigh-Bénard convection. The interest of our setup is that it gives straightforward information concerning the amplitude of the convective flow. In particular, we have shown that the spatial dependence of the velocity—at the midheight of the layer—is in total agreement with the theoretical predictions.

The results we obtained on the critical exponent are not complete at this moment, but some more sophisticated experiments are now in progress in our laboratory in order to understand the systematic departure from the theoretically predicted value 0.5.

The authors wish to thank Professor M. G. Velarde for his helpful assistance, Dr. Y. Pomeau for his constant interest and stimulating discussions, and Professor E. L. Koschmieder for valuable advice.

¹A recent compilation of the literature has been made by M. G. Velarde, in "Hydrodynamics," edited by R. Bahian (Gordon and Breach, New York, to be published); E. L. Koschmieder, *Beitr. Phys. Atmos.* **39**, 1 (1966); K. Stork and O. Müller, *J. Fluid Mech.* **54**, 599 (1972); G. Charlson and R. L. Sani, *Int. J. Heat Mass Transfer* **13**, 1479 (1970); E. L. Koschmieder, to be published;

A. I. Leont'yev and A. G. Kirdyashkin, *Heat Transfer—Sov. Res.* **1**, 5 (1969).

²M. J. Rudd, *J. Phys. E: J. Sci. Instrum.* **2**, 55 (1969).

³The theoretical value in the case of rigid-rigid boundaries and infinite geometry is 2.016, but experimentally in the case of finite geometry this value of r/d cannot be strictly followed as it has been clearly pointed out by S. H. Davis, *J. Fluid Mech.* **30**, 465 (1967), for example. At the onset of the convection, there must be an integral number of wavelengths.

⁴S. Chandrasekhar, *Hydrodynamic and Hydromagnetic Stability* (Clarendon, Oxford, England, 1961).

⁵We did not notice any change in the spatial position

of the maximum of V_z in the temperature range studied.

⁶We checked the reversibility of this characteristic.

⁷L. D. Landau, in *The Collected Papers of L. D. Landau*, edited by D. ter Haar (Gordon and Breach-Per-gamon, New York, 1965), p. 387.

⁸A comparison can also be made with the results found from the thermal variation of the Nusselt number, assuming that Nusselt number may be related to V_z^2 . We can note, however, that the Nusselt number depends on the geometry of the rolls (Koschmieder, Ref. 1) and that it is a very indirect parameter in the investigation of the local properties of the convective fluid. P. L. Silveston, *Forsch. Ingenieurw.* **24**, 29, 59 (1958).

Flute Instabilities during Fast Magnetic Compression of Collisionless $\beta = 1$ Plasmas

M. Keilhacker, M. Kornherr, H. Niedermeyer, F. Söldner, and K.-H. Steuer
Max-Planck-Institut für Plasmaphysik, Garching bei München, Germany*

(Received 29 January 1974)

End-on framing photographs taken at the Garching 500-kV theta pinch during fast magnetic plasma compression [$n_0 = (1.5-4) \times 10^{13} \text{ cm}^{-3}$] show distinct radial filaments that are due to flute instabilities of high azimuthal-mode number. The observed wavelengths are of the order c/ω_{p_i} ; they decrease with increasing density, but no mass dependence is found. The flute instabilities are responsible for the existence of a plasma halo which surrounds the thermonuclear $\beta = 1$ plasma column and has a major influence on its behavior.

Fast magnetic compression is as yet the most effective way of heating high- β plasmas to thermonuclear temperatures. Recent theoretical works^{1,2} indicate that shock-heated plasmas in toroidal systems can be stabilized against the dangerous $m = 1$ mode by the wall effect. The wall stabilization, however, becomes substantial only for high- β plasmas with small compression ratios. This means that the time for energy input is limited to the short period of shock compression. In order to transfer as much energy as possible to the plasma during implosion, it is necessary to have high current densities at the plasma surface and strong acceleration of the ions. High drift velocities in the magnetic piston excite microinstabilities which, on the one hand, lead to strong collisionless electron heating and, on the other, lead to enhanced field diffusion, and hence to broadening of the piston. Apart from microinstabilities, acceleration of the initial plasma produces macroinstabilities which result in a roughening of the plasma boundary and reduce the effective plasma compression.

The development of Rayleigh-Taylor instabilities in magnetically accelerated plasmas has already been observed in "collision-dominated

pinches."³ Wavelengths and growth rates of these instabilities were discussed from a magnetohydrodynamic point of view and the results agree very well with the observed values. In a collisionless plasma, however, particle interactions are long ranged and a fluid approximation would seem suspect. Up to now, only in the cases of appreciable trapped reversed magnetic fields were flute instabilities in collisionless shocks observed. In consequence of the bias fields these compression experiments lead only to ion temperatures of about 100 eV and rather low β values.⁴ To reach keV ion temperatures at high β values—the aim of high- β stellarator experiments—it is necessary to compress magnetic-field-free plasmas.

This paper describes observations of macroinstabilities during fast shock compression within an enlarged parameter range, and the scaling of the corresponding wavelengths. The experimental conditions and the regime of plasma parameters we have investigated are similar to those of planned high- β stellarator experiments. Therefore the results have a bearing on high- β confinement experiments which are based on the wall stabilization of weakly compressed plasmas.